

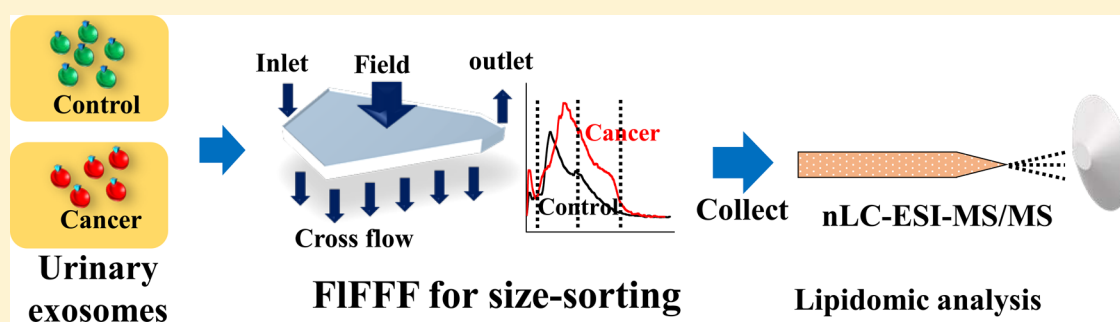
# Size Dependent Lipidomic Analysis of Urinary Exosomes from Patients with Prostate Cancer by Flow Field-Flow Fractionation and Nanoflow Liquid Chromatography-Tandem Mass Spectrometry

Joon Seon Yang,<sup>†</sup> Jong Cheol Lee,<sup>†</sup> Seul Kee Byeon,<sup>†</sup> Koon Ho Rha,<sup>\*,‡</sup> and Myeong Hee Moon<sup>\*,†</sup> 

<sup>†</sup>Department of Chemistry, Yonsei University, 50 Yonsei-Ro, Seoul, 03722 South Korea

<sup>‡</sup>Department of Urology, Yonsei University College of Medicine, 50-1 Yonsei-Ro, Seoul, 03722 South Korea

## Supporting Information



**ABSTRACT:** Exosomes are membrane-bound extracellular vesicles involved in intercellular communication and tumor cell metastasis. In this study, flow field-flow fractionation (FiFFF) was utilized to separate urinary exosomes by size, demonstrating a significant difference in exosome sizes between healthy controls and patients with prostate cancer (PCa). Exosome fractions of different sizes were collected for microscopic analysis during an FiFFF run and evaluated with exosome marker proteins using Western blot analysis. The results indicated that exosomes of different sizes originated from different types of cells. Collected exosome fractions were further examined using nanoflow ultrahigh performance liquid chromatography-electrospray ionization-tandem mass spectrometry (nUPLC-ESI-MS/MS) for lipidomic analysis. A total of 162 lipids (from 286 identified) were quantified using a selected reaction monitoring (SRM) method. The overall amount of lipids increased by 1.5- to 2-fold in patients with PCa and degree of increase was more significant in the smaller fractions (diameter <150 nm) than in the larger ones (diameter >150 nm) some classes of lipids. In addition, neutral lipids like diacylglycerol (DAG) and triacylglycerol (TAG) decreased in all exosomes without size dependency. Moreover, a dramatic increase in 22:6/22:6-phosphatidylglycerol (PG) was observed and significant decrease in (16:0,16:0)- and (16:1, 18:1)-DAG species (nearly 5-fold) and high abundant TAG species (>2.5-fold) was observed in patients with PCa. The results of this study indicate that FiFFF can be employed for the high-speed screening of urinary exosome sizes in patients with PCa and lipidomic analysis of the fractionated exosomes has potential for developing and distinguishing biomarkers of PCa.

Exosomes are membrane-bound extracellular vesicles (typically 30–100 nm in diameter) secreted by cells<sup>1–3</sup> that eliminate unnecessary molecules from cells and facilitate intercellular communication by transporting proteins, enzymes, RNA, and lipids to other cells.<sup>4</sup> Exosomes also promote tumor cell metastasis by transferring pathogenic proteins to nearby cells, a process that may also cause diseases such as Alzheimer's or prion disease.<sup>5,6</sup> Intercellular lipid transport by exosomes is of interest because exosomes carry bioactive lipids and enzymes related to lipid metabolism. Generally, the lipid composition of exosomes differs from that of the plasma membrane of parental cells because exosomes do not come from plasma membrane shedding but are secreted from late endosome compartments or vesicles called multivesicular bodies (MVB) in cells.<sup>1,7</sup> Compared to parental cells, they are generally enriched with sphingomyelin (SM), phosphatidylserine (PS), phosphatidylinositol (PI), phosphatidic acid (PA), ceramide (Cer), including

hexosylceramide (HxCer), and cholesterol.<sup>7,8</sup> Because exosomes carry bioactive lipids involved in inflammation and immunity, they can disturb target cell homeostasis.<sup>9,10</sup> Therefore, lipids characteristic of circulating exosomes can be utilized, along with protein and miRNA biomarkers, as biomarkers for diseases caused by lipid alteration.<sup>7</sup> However, the physiological function of exosomes is difficult to evaluate because it is difficult to distinguish exosomes from other microvesicles by size and protein composition. Moreover, exosomes in biological fluids such as blood and urine arise from a variety of cells with various functions.<sup>11,12</sup> Regarding urinary exosomes that may originate from the kidney, bladder, or prostate epithelial

**Received:** November 22, 2016

**Accepted:** January 19, 2017

**Published:** January 19, 2017

cells,<sup>13–15</sup> isolation of exosomes from high-abundance proteins is necessary to conduct proteomic and lipidomic analyses related to diseases.

Because exosomes from cancer cells contain pathogenic proteins related to cancer, biomarkers can be developed using exosomes from serum or urine and cancer cell lines. In the case of prostate cancer (PCa), a common cancer in men that is checked by measuring prostate-specific antigen (PSA) levels in the blood, new biomarker development is necessary because of the low specificity of a PSA-based diagnosis.<sup>16,17</sup> In particular, urine from PCa patients contains exosomes with several types of membrane vesicles and biomarker candidates that are distributed differently according to exosome size,<sup>18–20</sup> suggesting the importance of size-dependent analysis of exosomes.

Flow field-flow fractionation (FIFFF), an elution-based separation method, is capable of size-fractionating nanometer- to micrometer-sized particulate materials.<sup>21,22</sup> As the separation in FIFFF is performed in an unobstructed channel using the interaction of two flow streams, a migration flow moving along the channel axis toward a detector and a crossflow moving across a thin rectangular channel, the shear-induced degradation or loss of samples from unwanted interaction with the stationary phase (as in chromatography) is minimized. Size separation of sample components is achieved in an increasing order of molecular weight or hydrodynamic diameter. Because particles of a small diameter diffuse faster and extrude further away from the channel wall than those of a large diameter when crossflow is applied across the channel, the smaller particles migrate at higher speeds than the large particles owing to the parabolic velocity profile of movement in a thin channel. Due to the biocompatible features, such as being free of packing materials and organic solvents, FIFFF has been powerfully applied to various biological species, including proteins, ribosomal subunits, subcellular species (organelles), lipoproteins, and cells.<sup>23–30</sup> In particular, FIFFF was utilized for exosome separation from human neural stem cells prior to proteomic analysis.<sup>31</sup> Furthermore, FIFFF was used to characterize exosome size in mouse melanoma cell lines<sup>32</sup> and lyophilized exosome standards<sup>33</sup> using multiangle light scattering.

In this study, FIFFF was utilized for the size fractionation of urinary exosomes from PCa patients. Additionally, fractions of exosome with narrow diameters were further investigated for size-dependent quantitative lipidomic analysis in comparison to those from healthy controls by nanoflow ultrahigh performance liquid chromatography-electrospray ionization-tandem mass spectrometry (nUPLC-ESI-MS/MS). Exosomes from human urine were size-sorted using an asymmetrical FIFFF (AF4) channel. Exosome fractions of different sizes were examined by transmission electron microscopy (TEM) and confirmed by Western blot analysis using exosome-specific markers. On the basis of Western blot results, exosomes were collected into two different sized fractions, which were further investigated to quantify the urinary exosomal lipids found in PCa patients and those found in healthy controls using selected reaction monitoring (SRM) of nUPLC-ESI-MS/MS. The present study demonstrated the potential of FIFFF for analyzing the particle size distribution of urinary exosomes and the size-dependent distribution of lipids in urinary exosomes from PCa patients compared to those from healthy controls.

## ■ EXPERIMENTAL SECTION

**Materials and Reagents.** Protein standards and chemicals were purchased from Sigma-Aldrich (St. Louis, MO, USA): thyroglobulins (670 kDa), methyl *tert*-butyl ether (MTBE), Triton X-100, Tween-20, urea, and dithiothreitol (DTT). Polystyrene standards with nominal diameters of 46, 102, and 203 nm were purchased from Thermo Fisher Scientific (Waltham, MA, USA). Primary (rabbit- $\alpha$ -CD9, rabbit- $\alpha$ -ALIX, and rabbit- $\alpha$ -CD46) and secondary (antirabbit-IgG (HRP-linked)) antibodies were purchased from Abcam Plc. (Cambridge, UK) and Cell Signaling Technology, Inc. (Danvers, MA, USA), respectively. EZ-Western Lumi Femto solution was purchased from Daeil Lab Service Co. Ltd. (Seoul, Korea) for chemiluminescence detection. High performance liquid chromatography (HPLC) solvents were purchased from J.T. Baker, Inc. (Phillipsburg, NJ, USA): water, acetonitrile (ACN), methanol, and isopropanol (IPA). Fifteen lipid standards having odd numbered acyl chains used in a mixture of internal standards (ISs) for the quantification of exosomal lipids were purchased from Avanti Polar Lipid, Inc. (Alabaster, AL, USA): 17:0-lysophosphatidylcholine (LPC), 13:0/13:0-phosphatidylcholine (PC), 17:1-lysophosphatidylethanolamine (LPE), 17:0/17:0-phosphatidylethanolamine (PE), d18:1/17:0-SM, 17:0/17:1/17:0-triacylglycerol-*d*<sub>5</sub> (TAG), d18:1/17:0-monoheptacosylceramide (MHC), d18:1/17:0-Cer, 17:1-lysophosphatidylglycerol (LPG), 15:0/15:0-phosphatidylglycerol (PG), 17:1-lysophosphatidylserine (LPS), 17:0/20:4-PS, 17:0-lysophosphatidylacid (LPA), 17:0/17:0-PA, and 17:0/20:4-PI.

**Collection of Urine Samples and Isolation of Exosomes.** Urine samples of healthy controls (approximately 100 mL each) were obtained from 28–30 year old healthy volunteers in the morning after a 12 h fast. Those from PCa patients were collected prior to prostatectomy with approval of the Institutional Review Board (IRB) from Severance Hospital (Seoul, Korea) from patients who were diagnosed as positive by biopsy. Urine samples were combined with cOmplete Protease Inhibitor Cocktail tablets (1 tablet/50 mL; Roche, Indianapolis, IN, USA) within 1 h after collection and stored at  $-80^{\circ}\text{C}$ . Exosomes were isolated from urine using a differential centrifuge method as follows: 50 mL of urine was centrifuged at 12 000g and  $4^{\circ}\text{C}$  for 10 min to sink cell debris. The resulting supernatant was transferred to a tube for ultracentrifugation at 200 000g and  $4^{\circ}\text{C}$  for 1 h using an Optima LE-80K Ultracentrifuge (Beckman Coulter Inc., Brea, CA, USA). Thereafter, the supernatant was removed, and the exosome pellet was resuspended in 500  $\mu\text{L}$  of 0.1 M phosphate buffered saline (PBS) solution and vortexed for 20 min to completely disperse the exosomes.

**FIFFF.** An AF4 channel (model LC, 275 mm long) was utilized with a Nadir regenerated cellulose membrane (MWCO 10 kDa), both from Wyatt GmbH (Dernbach, Germany). The channel spacer was made from a 190  $\mu\text{m}$  thick Teflon sheet cut to 26.6 cm in length and 2.2 cm in initial breadth with a trapezoidal decrease to a final breadth of 0.6 cm. Samples were injected using a model 7125 injector (Rheodyne, Cotati, CA, USA) with a 50  $\mu\text{L}$  sample loop in the focusing/relaxation mode, in which the two flow streams from both the inlet and the outlet of the channel were focused at a 1/10 position from the channel inlet by rotating the two valves (4-way and 3-way) as illustrated elsewhere.<sup>30</sup> The total flow rate was maintained at 3 mL/min for 5 min for sample injection and simultaneous focusing/relaxation. Thereafter, the two valves were rotated so

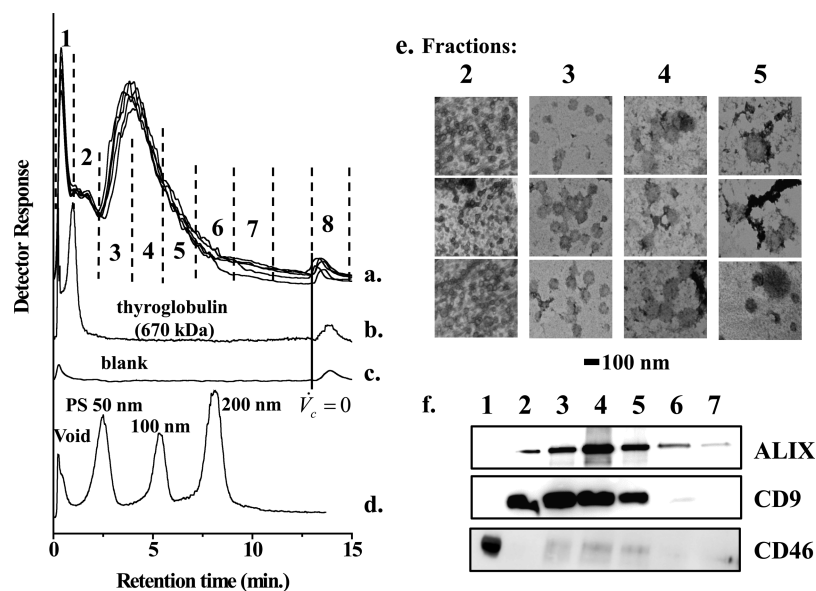


**Figure 1.** AF4 fractograms of (a) urinary exosomes from a healthy control (five repeated runs), (b) thyroglobulin, (c) a blank run, and (d) PS standard mixtures (50, 100, and 200 nm); (e) TEM images of collected fractions (2–5); (f) Western blot results of collected exosome fractions. Separation was achieved at a channel outflow rate of 1.8 mL/min and a crossflow rate of 1.2 mL/min, which was dropped to 0 mL/min at 13 min in runs a–c. Carrier solutions were 0.1 M PBS for runs a–c and 0.1% FL-70 with 0.02%  $\text{NaN}_3$  for run d.

that all flows entered the channel inlet for separation at flow rate conditions (outflow rate = 1.8 mL/min and crossflow rate = 1.2 mL/min). Carrier liquids for FIFFF were made from Ultrapure water (>18 M $\Omega$ -cm) containing 0.1 M PBS solution for exosome samples or 0.1% FL-70 with 0.02%  $\text{NaN}_3$  as bactericide for polystyrene standards. All carrier solutions were filtered through a 0.22  $\mu\text{m}$  nitrocellulose membrane filter from EMD Millipore (Billerica, MA, USA). Carrier liquid was delivered to the AF4 channel, and exosomes were detected using a model SP930D HPLC pump and a model UV730D UV–vis detector at 280 nm, respectively (Young-Lin Instruments, Seoul, Korea). Detector signals were recorded by Autochro-Win 2.0 plus software (Young-Lin). Exosome fractions were collected during AF4 separation for further examination with a TEM, by Western blot, and for proteomic and lipidomic analysis.

**TEM Analysis of Exosomes.** Exosome fractions were collected during AF4 separation (five repeated runs) over a time interval of 1 min for fraction 1 and 1.5 min for fractions 2–5 (Figure 1a). Each fraction was concentrated to a final volume of 50  $\mu\text{L}$  by sequential enrichment using an Amicon Ultra-15 Centrifugal Filter (30 kDa NMWL) and Amicon Ultra 0.5 mL vial (100 kDa NMWL) from EMD Millipore. TEM analysis was performed by negative staining using a model JEM-1011 transmission electron microscope (JEOL Ltd., Tokyo, Japan). A 10  $\mu\text{L}$  portion of each concentrated exosome fraction was placed on a Formvar stabilized with carbon film on 300 mesh copper grids (Ted Pella Inc., Redding, CA, USA) and fixed for 2 min. The water drop was then removed using filter paper. Before the specimen dried up completely, 2  $\mu\text{L}$  of 2% uranyl acetate solution (Ted Pella Inc.) was applied to the exosomes for 1 min for negative staining. Thereafter, the droplet was removed using filter paper, and the specimen was allowed to dry for 30 min.

**Western Blot Analysis of Exosome Fractions.** AF4 fractions were examined using Western blot analysis. Each fraction was concentrated to a volume of approximately 250  $\mu\text{L}$  using Amicon Ultra-15 Centrifugal Filters. The resulting

solution was tip-sonicated (pulse durations of 10 s with 2 s intervals) for 5 min to lyse exosomes for the Bradford assay. On the basis of the measured amount of protein in each fraction, a portion of the exosome solution equivalent to 5  $\mu\text{g}$  of proteins was mixed with 5 $\times$  Laemmli buffer solution (pH 6.8) at 90  $^\circ\text{C}$  for 5 min to denature the proteins. Electrophoresis was carried out on a 10% polyacrylamide gel using a Mini-PROTEAN Tetra Cell System (Bio-Rad Laboratories, Inc., Hercules, CA, USA) with applied voltages of 80 V in the stacking gel and 150 V in the running gel. After electrophoresis, proteins were transferred to polyvinylidene difluoride (PVDF; pore size of 0.45  $\mu\text{m}$ ) transfer membranes (Bio-Rad Laboratories) at 200 V for 1 h. Membrane blocking was performed using blocking solution (5% (w/v) skim milk in tris-buffered saline plus Tween (TBS-T)) for 1 h at room temperature; then, the solution was incubated with antibody for 1 h at room temperature. Stained bands were detected using chemiluminescence detection with an LAS-4000 mini Detector (GE Healthcare, Little Chalfont, UK).

**Lipid Extraction from Exosomes in AF4 Fractions.** Extraction of lipids from urinary exosomes in AF4 fractions was performed on the basis of the Folch method modified with MTBE/ $\text{CH}_3\text{OH}$ .<sup>34</sup> The concentrated exosome solution of each fraction (reduced to approximately 250  $\mu\text{L}$ ) was placed in a 2 mL centrifuge tube and mixed with 300  $\mu\text{L}$  of  $\text{CH}_3\text{OH}$ . The tube was then immersed in an ice water bath for 10 min. One milliliter of MTBE was added, and the mixture was vortexed for 5 min. The upper organic layer was placed in another 2 mL tube, and the remaining aqueous layer was mixed with 500  $\mu\text{L}$  of MTBE/ $\text{CH}_3\text{OH}$  (10:3, v/v) and vortexed for 10 min. The upper layer was taken and combined with the previously collected organic layer. This process was repeated twice. The top of the tube containing the final organic extracts was wrapped with a 0.45  $\mu\text{m}$  MillWrap PTFE membrane (EMD Millipore) to protect against evaporation of lipid molecules. The solution was lyophilized to dryness overnight using a Bondiro MCFD 8508 freeze-drying vacuum centrifuge (Ilshin Lab Co., Yangju, Korea). The dried lipids were weighed and

reconstituted in  $\text{CHCl}_3/\text{H}_2\text{O}$  (1:1, v/v) to a final lipid concentration of  $5 \mu\text{g}/\mu\text{L}$ . Finally, the mixture of 15 lipid ISs was added to a concentration of  $0.3 \text{ pmol}/\mu\text{L}$  for each IS, and the solution was stored in a refrigerator at  $4^\circ\text{C}$ .

**nUPLC-ESI-MS/MS of Exosomal Lipids.** A Dionex Ultimate 3000 RSLCnano LC System coupled to an LTQ Velos ion trap mass spectrometer from Thermo Scientific (San Jose, CA, USA) was used for the nontargeted lipid analysis. A pulled-tip capillary column ( $7 \text{ cm} \times 100 \mu\text{m}$ , i.d.) was prepared in the laboratory by packing  $1.7 \mu\text{m}$  ethylene-bridged hybrid (BEH) C18 particles ( $130 \text{ \AA}$ ) unpacked from a BEH C18 column (Waters, Milford, MA, USA) for nUPLC separation. A detailed procedure for column packing can be found in the literature.<sup>30</sup> For nUPLC-ESI-MS/MS analysis,  $3 \mu\text{L}$  of the final lipid suspension ( $15 \mu\text{g}$  of lipids with  $0.9 \text{ pmol}$  of each IS) was injected for both positive and negative ion modes of MS. Mobile phase solutions for lipid analysis were  $\text{H}_2\text{O}/\text{ACN}$  (9:1, v/v) for A and  $\text{CH}_3\text{OH}/\text{ACN}/\text{IPA}$  (2:2:6, v/v/v) for B. Both were added with a mixed modifier ( $5 \text{ mM HCO}_2\text{NH}_4$  and  $0.05\% \text{ NH}_4\text{OH}$ ), which was effective for the ionization of lipid molecules in both positive and negative ion modes.<sup>35</sup> Sample loading was performed with 99% A for 10 min at  $800 \text{ nL}/\text{min}$ . After sample loading, the column flow rate was adjusted to  $350 \text{ nL}/\text{min}$  with the split flow valve at a pump flow rate of  $5 \mu\text{L}/\text{min}$  in such a way as to reduce dwell time. Gradient elution began by ramping to 40% B for 1 min and increasing to 80% B for 10 min and further to 99% B for 20 min. This was maintained for 15 min and then returned to 1% B for column reconditioning. The precursor scan was monitored in the  $m/z$  range of  $350\text{--}1100 \text{ Da}$  with the ESI voltage at  $3.0 \text{ kV}$  for both ion modes. Some classes of lipids (PC, PEp, SM, Cer, MHC, DAG, TAG, and ChE) were identified in positive ion mode using data dependent MS/MS experiments, and the remaining classes (PI, PG, PS, PA, and PE) were identified in negative ion mode. Structural identification of lipids was performed using LiPilot,<sup>36</sup> a computer-based algorithm, followed by manual confirmation of the structures.

For quantitation of lipids, nanoACQUITY UPLC System (Waters) coupled with a TSQ Vantage triple-stage quadrupole mass spectrometer (Thermo Scientific) was employed to quantify the lipids. The same analytical column utilized for lipid identification was used along with the same mobile phases except gradient elution conditions. Sample loading was performed with mobile phase A at  $1 \mu\text{L}/\text{min}$  for 10 min. After loading, the pump flow rate was increased to  $20 \mu\text{L}/\text{min}$  with the split valve on so that the column flow rate was adjusted to  $500 \text{ nL}/\text{min}$ . Gradient elution began by increasing B to 80% for 5 min and further to 100% for 10 min. Thereafter, it was maintained at 100% B for 10 min and returned to 100% A, followed by 5 min of column reconditioning. Lipid ions identified from the nontargeted analysis were quantified using the SRM method. The types of precursor ions and quantifier ions for the 15 lipid categories utilized for the SRM quantitation are listed in Table S1. Quantitation was based on the calculation of relative peak areas compared to each IS ( $250 \text{ fmol}/\mu\text{L}$ ) added to the lipid extract samples. The molecular structures of the ISs are listed in Table S1.

## RESULTS AND DISCUSSION

**AF4 Separation of Urinary Exosomes.** Isolated exosomes were examined first in a healthy normal urine sample using AF4 separation, followed by Western blot to confirm the exosomes. Figure 1 shows the fractograms of (a) the resuspended

exosome sample (the injection volume was  $25 \mu\text{L}$ , equivalent to  $2.5 \text{ mL}$  urine) to the AF4 system obtained from five repeated runs, (b) thyroglobulin ( $670 \text{ kDa}$ ) as a protein standard, (c) a blank injection, and (d)  $2 \mu\text{L}$  of each polystyrene standard ( $50$ ,  $100$ , and  $200 \text{ nm}$ ,  $1\% \text{ w/v}$ ) along with (e) the TEM images and (f) Western blot results of the exosome fractions collected at the time intervals of 1 min for fraction 1, 1.5 min for fractions 2–5, and 2 min for fractions 6–8. All runs in Figure 1a–d were obtained at an outflow rate of  $1.8 \text{ mL}/\text{min}$  and a crossflow rate of  $1.2 \text{ mL}/\text{min}$ . For runs a–c, the crossflow rate was reduced to  $0 \text{ mL}/\text{min}$  at 13 min to confirm any material dragged at the channel surface. Therefore, small peaks were observed after approximately 13 min; these were the system pulses generated from the change in channel pressure. From the retention times of the polystyrene standards, the size of the urinary exosomes was estimated to be approximately  $50\text{--}200 \text{ nm}$ . TEM micrographs of the four fractions (2–5) indicated that the exosome size increased as the fraction number increased. Table 1 lists the average diameter for each fraction. The results

**Table 1. Average Exosome Diameter in Each Fraction Based on the TEM Images in Figure 1**

fraction #	time (min)	diameter (nm)	counted numbers
2	1.0–2.5	$28.2 \pm 4.3$	23
3	2.5–4.0	$65.3 \pm 6.7$	14
4	4.0–5.5	$87.8 \pm 16.1$	16
5	5.5–7.0	$136.7 \pm 27.9$	11

indicated that the exosomes were well fractionated in an increasing order of diameter. Fraction 1 displayed an intense, but somewhat broad, peak at the very beginning of elution while void peaks were typically observed in the runs b and c. Fraction 1 is supposed to contain proteins smaller than thyroglobulin, which were not removed completely during the isolation process. To confirm the presence of exosomes in different retention time regions, collected fractions were further analyzed by Western blot using ALIX and CD9 antibodies, both of which are exosome markers, and CD46 antibody, a prostatic marker or plasma membrane protein.<sup>37</sup> The Western blot results from the seven fractions (Figure 1f) indicated that fraction 1 did not respond to the two exosomal markers, but to CD46, which indicated that fraction 1 consisted of membrane proteins, including membrane debris. Though both ALIX and CD9 are exosome markers, ALIX is known to exist in MVB only and CD9, a membrane protein, exists at the membrane surface. From the Western blot, exosomes in fractions 2–5 responded to both markers, but the larger exosomes in fractions 6 and 7 responded to ALIX only. This observation indicated that exosomes larger than approximately  $150 \text{ nm}$  were not composed of exosomes with CD9, which are known to originate from immune cells involved in the formation of lymphocytes, such as B-cells.<sup>38</sup> Therefore, exosomes that originated from immune cells were differentially fractionated from those that originated from prostate and kidney cells.

On the basis of the initial evaluation of exosome fractions in Figure 1, the exosome retention profiles of patients with PCa and those of healthy controls were compared by injecting the same volume ( $25 \mu\text{L}$ ) of exosome suspension, but in this case, each urine sample was pooled from the four patients with PCa and the four controls, respectively (Figure 2). The retention profile of the pooled exosomes from patients with PCa

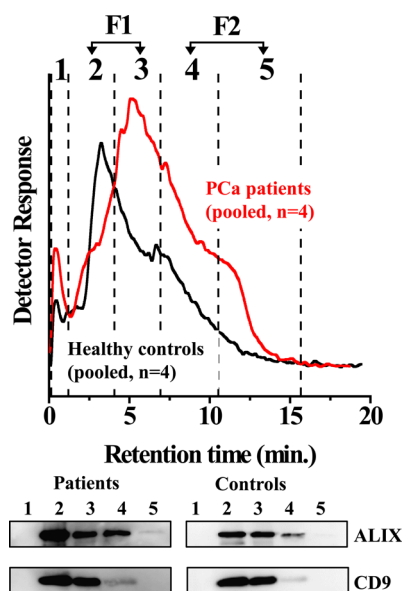


**Figure 2.** Fractograms of urinary exosomes from the pooled urine samples of four prostate cancer patients and four healthy controls, respectively, and Western blot results of the collected fractions. Collection periods were as follows: fraction 1: 0.25–1.0 min, 2: 1.0–4.0 min, 3: 4.0–7.0 min, 4: 7.0–10.5 min, and 5: 10.5–16.5 min.

appeared to be clearly different from that pooled from the healthy controls. There was an increase in peak intensity and a shift in the maximum retention time, which corresponded to an increase in exosome size at the maximum population: 107.3  $\mu\text{m}$  for PCa patients and 58.3  $\mu\text{m}$  for controls based on the diameter calculation from retention time using FIFFF theory.<sup>22</sup> Individual urinary exosome samples were analyzed using AF4 separation to evaluate variations among individuals (Figure S1). Patterns of retention and size distribution were similar, but there were slight variations in exosome concentration among individuals. To the best of our knowledge, this was the first time a study has distinguished a clear difference in urinary exosome size distribution between patients with PCa and healthy controls. By comparing the Western blot results of the five fractions collected during AF4 separation, we found that CD9 was not detected in the larger exosome particles (fractions 4 and 5) from both patients and controls, whereas ALIX was detected in fractions 2–4 for both groups, but not in fraction 5. Similar to the larger exosomes (fractions 6 and 7) in Figure 1, the absence of CD9 in fractions 4 and 5 for both groups supported that, regardless of the development of PCa, large size exosomes may originate from different cellular origins compared to small size exosomes that were related to prostate and kidney cells. After multiple Western blot analyses of fractions collected at different time intervals (not shown here), fractions 2 and 3 were selected to be combined as F1 and fractions 4 and 5 were combined as F2 for further lipidomic analysis between the two distinct size groups of exosomes (smaller and larger than approximately 150 nm in diameter) (Figure 2).

**Lipidomic Analysis of Urinary Exosomes from Patients with PCa.** For lipid analysis of the two exosome fractions (smaller or larger than approximately 150 nm), 25  $\mu\text{L}$  of exosome suspension from the pooled urine samples was injected 10 times to accumulate sufficient exosome particles for lipid extraction. For comparison, 250  $\mu\text{L}$  of the original exosome suspension from each group was used for lipid

extraction. Lipid analysis was performed using a nontargeted search first using nUPLC with ion trap MS and followed by targeted SRM quantitation using nUPLC with triple quadrupole MS. The performance of lipid separation utilized in this study was demonstrated with the base peak chromatograms (BPCs) of the 15 lipid standards in both positive and negative ion modes of nUPLC-ESI-MS/MS (Figure S2). For lipid extracts from urinary exosomes, 3  $\mu\text{L}$  of lipid extracts from each urinary exosome sample (adjusted to 5  $\mu\text{g}/\mu\text{L}$ ) was injected for both qualitative and quantitative analysis. BPCs of exosomal lipids from both the control and PCa groups are shown in Figure S3. From the nontargeted analysis, a total of 286 lipids (30 PC, 27 PE, 13 PEp, 11 PS, 13 PI, 9 PA, 15 PG, 14 SM, 6 Cer, 5 MHC, 8 ChE, 6 DAG, and 129 TAG) were identified from the unfractionated exosome extracts of healthy controls (278 lipids) and patients with PCa (278). Among these, 270 species were common to both groups. On the basis of the identified lipids, SRM quantitation was accomplished for only 164 lipids because lipids in the PC, PE, and TAG categories could only be quantified without differentiating isomeric structures. The average peak area ratio of patient to control (P/C) for each lipid species from triplicate measurements is listed in Table S2. The molecular structures of PC, PE, and TAG species identified from collision induced dissociation (CID) experiments are listed in Table S3. During the quantitative analysis of exosomal lipids, an SRM time table for a high-speed targeted analysis within 20 min per sample<sup>39</sup> was utilized to scan each individual molecule over 2 min intervals during nUPLC-ESI-MS/MS. The quantification results listed in Table S2 indicate the P/C ratios of corrected peak area (relative to 1 pmol of each IS, which is specific to each lipid class) along with the relative abundance of each lipid class, which was based on healthy controls. The underlined abundance values represent the high abundance species in each class, which was defined when the relative abundance of each species was larger than 100%/number of lipids in each class. Changes in the amount of each lipid class were plotted in Figure 3 by comparing the P/C ratio of the whole exosome, F1,

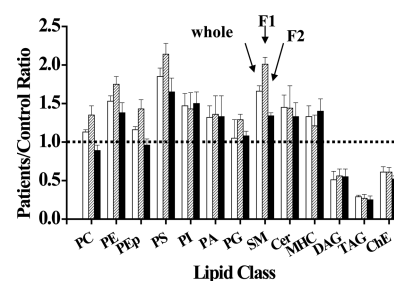


**Figure 3.** Changes in total amounts of each lipid class plotted as the patient/control (P/C) ratio of whole exosome pellets and size sorted fractions F1 and F2 obtained from Figure 2a.

and F2 fractions. The results indicated that the levels of most lipid classes, except DAG, TAG, and ChE, increased in patients with PCa compared to those of healthy controls. General increases of phospholipids in the exosomes from patients with PCa may have originated from the increased expression of fatty acid synthase (FAS) in cancer cells,<sup>40</sup> which promotes the synthesis of fatty acids in cancer cells as they grow. However, the decrease in the TAG level may have arisen from the increased consumption of energy during cancer progression through the metabolic process.<sup>40</sup> In addition, the decrease in

Table 2. Lipids Showing Significant Changes ( $P/C > 2.5$  and  $p < 0.01$ ) in Either the Whole Exosome or Collected Fractions (F1 and F2) by AF4 Separation Using nUPLC-ESI-MS/MS (Triplicate Measurements) Represented with the Relative Abundance (%) in Each Lipid Class<sup>a</sup>

class	increased species				decreased species								
	molecular species	m/z	%	whole (P/C)	F1(P/C)	F2(P/C)	class	molecular species	m/z	%	whole (P/C)	F1(P/C)	F2(P/C)
PC	18:1	522.5	1.3	2.58 ± 0.22	1.98 ± 0.71	2.67 ± 0.16	PE	36:4	740.2	8.9	0.25 ± 0.03	0.55 ± 0.05	0.33 ± 0.06
	34:1	760.3	14.0	2.32 ± 0.21	2.67 ± 0.39	2.11 ± 0.18		36:3	742.4	7.0	0.32 ± 0.04	0.52 ± 0.09	0.31 ± 0.08
	44:12	878.2	0.0	8.17 ± 3.65	8.40 ± 6.03	5.25 ± 2.72		38:4	768.5	13.2	0.34 ± 0.03	0.64 ± 0.09	0.31 ± 0.08
PE	16:0	454.1	4.6	2.62 ± 0.43	4.86 ± 0.71	2.39 ± 1.85	PI	16:0/18:2	833.7	12.7	0.20 ± 0.11	0.17 ± 0.06	0.38 ± 0.24
	18:0	482.3	18.7	2.89 ± 0.08	2.88 ± 0.30	2.68 ± 0.50	DAG	16:0,16:0	586.4	37.4	0.56 ± 0.15	0.58 ± 0.18	0.37 ± 0.07
	20:1	508.5	1.3	2.89 ± 1.55	3.78 ± 0.93	2.93 ± 0.42		16:1,18:2	608.4	3.1	0.01 ± 0.01*	0.01 ± 0.01*	0.01 ± 0.01*
PEp	36:2	744.6	9.2	2.14 ± 0.15	2.56 ± 0.24	1.83 ± 0.47		16:1,18:1	610.4	46.8	0.17 ± 0.06	0.18 ± 0.14	0.17 ± 0.17
	p16:0/20:5	722.6	3.8	2.13 ± 0.35	3.22 ± 0.31	1.32 ± 0.09		18:0,20:4	662.6	3.6	1.14 ± 0.57*	0.35 ± 0.31*	1.11 ± 0.25*
	p16:0/20:3	726.7	1.3	2.21 ± 0.23	3.38 ± 0.47	1.57 ± 0.10	TAG	46:3	790.6	0.4	0.39 ± 0.37*	0.11 ± 0.03*	0.04 ± 0.04*
PS	p16:0/22:6	748.6	6.0	2.07 ± 0.15	3.25 ± 0.56	1.24 ± 0.13		46:2	792.8	3.2	0.20 ± 0.03	0.16 ± 0.04	0.11 ± 0.04
	16:0	496.4	1.5	4.74 ± 1.75	5.13 ± 3.75	4.28 ± 2.72		46:1	794.7	6.6	0.27 ± 0.08	0.20 ± 0.05	0.37 ± 0.02
	18:1	522.3	3.8	2.91 ± 0.76	4.40 ± 2.06	2.17 ± 0.61*		46:0	796.7	0.6	0.24 ± 0.08*	0.10 ± 0.04*	0.57 ± 0.30*
PI	16:0/18:1	760.7	17.9	2.03 ± 0.19	2.58 ± 0.38	1.88 ± 0.18		48:3	818.7	0.2	0.20 ± 0.07	0.19 ± 0.06	0.03 ± 0.06
	18:0/18:2	786.7	6.8	2.60 ± 0.46	3.24 ± 0.44	2.01 ± 0.25		48:2	820.8	3.9	0.06 ± 0.01	0.11 ± 0.03	0.10 ± 0.03
	18:0/20:4	810.7	8.3	3.47 ± 0.76	3.14 ± 0.72	3.47 ± 1.51		48:1	822.8	0.6	0.06 ± 0.01	0.08 ± 0.04	0.10 ± 0.02
PA	18:1	597.4	3.5	3.77 ± 1.10	4.53 ± 1.62	3.03 ± 0.97		48:0	824.4	17.4	0.24 ± 0.11	0.23 ± 0.16	0.21 ± 0.01
	18:0	599.4	44.5	2.45 ± 0.49	3.24 ± 0.90	2.20 ± 0.29		50:3	846.8	0.1	0.24 ± 0.11	0.15 ± 0.05	0.13 ± 0.10
	18:1/18:1	861.7	0.7	3.40 ± 0.67	4.29 ± 1.14	1.71 ± 0.42		50:2	848.7	1.4	0.11 ± 0.03	0.10 ± 0.03	0.09 ± 0.02
PG	18:1/18:1	699.4	9.2	1.80 ± 0.52	3.21 ± 1.36	2.00 ± 0.34		50:1	850.8	5.5	0.44 ± 0.05	0.53 ± 0.07	0.12 ± 0.02
	18:0/20:4	723.7	19.4	2.90 ± 0.11	3.09 ± 0.25	2.51 ± 0.18		50:0	852.8	3.5	0.45 ± 0.17	0.11 ± 0.01	0.11 ± 0.02
	22:6/22:6	865.8	9.7	4.76 ± 0.16	7.58 ± 0.15	3.39 ± 0.26		52:5	870.7	1.4	0.44 ± 0.04	0.52 ± 0.23	0.32 ± 0.30
SM	18:1/20:4	795.7	0.3	1.90 ± 0.80*	3.00 ± 0.87	2.29 ± 0.62*		52:4	872.8	8.9	0.49 ± 0.11	0.72 ± 0.14	0.46 ± 0.08
	d18:1/14:0	675.7	0.5	2.31 ± 1.03	3.27 ± 0.32	1.64 ± 0.20		52:3	874.8	7.3	0.39 ± 0.14	0.30 ± 0.09	0.23 ± 0.04
	d18:1/18:1	729.5	1.7	1.40 ± 0.16	2.51 ± 0.25	0.87 ± 0.08		52:2	876.9	1.4	0.47 ± 0.06	0.72 ± 0.14	0.46 ± 0.08
MHC	d18:1/20:0	759.9	8.1	2.71 ± 0.16	3.24 ± 0.29	2.47 ± 0.17		52:1	878.9	1.6	0.43 ± 0.39*	0.19 ± 0.02*	0.15 ± 0.01*
	d18:1/24:2	811.7	0.8	2.46 ± 0.47	2.79 ± 0.32	1.12 ± 0.13		54:4	900.8	9.1	0.47 ± 0.08	0.35 ± 0.09	0.58 ± 0.17
	d18:1/24:1	813.6	7.6	2.46 ± 0.47	2.71 ± 0.35	1.72 ± 0.24		54:3	902.8	10.0	0.58 ± 0.04	0.26 ± 0.03	0.55 ± 0.09
Cer	d18:1/24:0	815.8	12.2	2.49 ± 0.29	3.27 ± 0.25	2.80 ± 0.22		54:2	904.9	1.9	0.55 ± 0.13	0.23 ± 0.03	0.19 ± 0.05
	d18:1/16:0	700.6	11.6	3.60 ± 0.27	4.63 ± 0.13	2.81 ± 0.36		54:1	906.8	6.3	0.35 ± 0.19	0.26 ± 0.01	0.55 ± 0.03
	d18:1/20:0	756.6	12.1	2.04 ± 0.31	4.18 ± 1.21	3.17 ± 0.33		54:0	908.9	0.3	0.80 ± 0.40*	0.27 ± 0.05*	0.15 ± 0.03*
ChE	d18:1/18:0	566.7	3.8	4.50 ± 0.24	4.05 ± 0.54	3.16 ± 0.35		56:4	928.9	0.2	0.44 ± 0.44*	0.15 ± 0.06*	0.21 ± 0.04*
	d18:1/22:4	614.7	5.5	4.88 ± 1.39	12.13 ± 3.42	12.20 ± 2.36		56:3	930.8	0.3	0.48 ± 0.14*	0.10 ± 0.04*	0.14 ± 0.03*
	d18:1/24:1	648.8	38.6	2.51 ± 0.78	2.08 ± 0.27	3.04 ± 0.47	ChE	14:0	614.6	31.6	0.20 ± 0.05	0.13 ± 0.03	0.16 ± 0.02
	18:3	664.7	3.5	1.42 ± 0.15	4.00 ± 0.95	1.14 ± 0.11		16:0	642.6	40.2	0.25 ± 0.06	0.22 ± 0.06	0.20 ± 0.04

<sup>a</sup>Underlined species are high abundance species in each class. \* =  $p < 0.05$ .

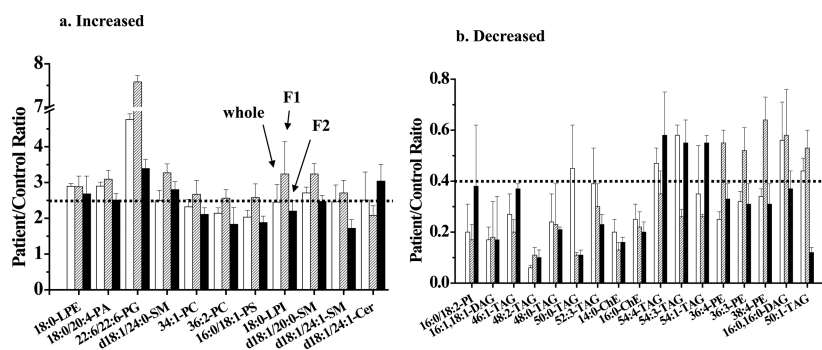


**Figure 4.** Patient/control (P/C) ratios of highly abundant lipid species with significant changes [(a)  $P/C > 2.5$ ; (b)  $P/C < 0.4$ ; both with  $p < 0.01$ ] in at least one fraction (F1 or F2) by FIFFF.

the ChE level in exosomes may have resulted from a decreased secretion from cancer cells.

This result was similar to a previous report in which ChE accumulated in prostate cancer cells during cancer progression.<sup>41</sup> Lipids in the PC, PE, PEp, PS, and SM classes increased more in the F1 fraction than in the F2 fraction (Figure 3). This indicated that those lipid classes were more enriched in the smaller exosomes, whereas other classes, including the three classes whose levels decreased, did not display a size dependent variation. Individual lipid species showing significant changes ( $P/C > 2.5$  or  $P/C < 0.4$ ,  $p < 0.01$ ) either in the whole exosome or in one of the fractions are listed in Table 2. P/C values of relatively high abundance species (underlined in Table 2) are plotted in Figure 4. Compared to the urinary exosomes of healthy controls, 22:6/22:6-PG showed an increasing pattern among patients with PCa (about 7.5 times in F1 and 3.4 times in F2), whereas most species shown in Figure 4a tend to increase by 2.5-fold. Among DAG species in Table 2, (16:0, 16:0)-DAG and (16:1, 18:1)-DAG, which together comprise more than 80% of the total DAG amount, showed a decreasing pattern (2–5-fold) in the urinary exosomes of patients with PCa compared to those of healthy controls. In the case of TAG, seven out of ten high abundance species tended to decrease by more than 2.5-fold in patients with PCa compared to healthy controls (Figure 4b).

Because an increased expression of FAS in cancer cells is known to catalyze the synthesis of palmitic acid (16:0), which further elongates to stearic acid (18:0) and oleic acid (18:1),<sup>40</sup> the relative changes in lipids containing these acyl chains was investigated. In particular, PS, which displayed the largest increase among phospholipid classes in Figure 3, is related to the development of cancer because all 11 PS molecules (Table S2) contained at least one of these three acyl chains. In addition, PS levels showed increasing tendency with PCa, except 18:0-LPS, 18:0/18:0-PS, and 18:1/18:1-PS (Figure 5). 16:0-LPS and 18:1-LPS showed significant increases (>4-fold) in the F1 fractions of patients with PCa compared to those of healthy controls. Though PS on the cell surface is known to trigger phagocytes to engulf apoptotic cells, PS contained in exosomes may play a role as a mediator of cell-to-cell interactions and, therefore, may affect the immune system.<sup>42</sup> In particular, the expression of PS in PCa cells can be utilized as a marker of cancer metastasis.<sup>43</sup> Therefore, increases in PS levels in the exosomes from patients with PCa resulted from an increase in FAS in cells and from cancer metastasis. Most PS levels increased in the F1 fraction more than in the F2 fraction; however, there was no size dependent variation in 18:0-LPS, 18:0/18:0-PS, 18:0/20:4-PS, and 18:1/18:1-PS. Among these,

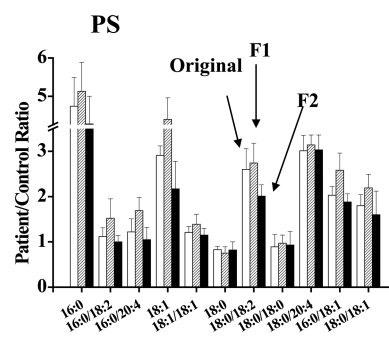


**Figure 5.** Changes in patient/control (P/C) ratio of exosomal PS species having one of the three fatty acyl chains (16:0, 18:0, and 18:1) involved in the overexpression of fatty acid synthase (FAS) in prostate cancer.

18:0-LPS and 18:0/18:0-PS showed negligible changes in PCa patients compared to healthy controls. Because changes in exosomal lipid levels were greater in the smaller size exosomes (<150 nm) than in the larger ones (>150 nm), larger exosomes may originate from different types of cells during the PCa progression.

## CONCLUSIONS

This study demonstrated that FIFFF can be utilized to separate exosomes by size, to determine the size distributions of urinary exosomes derived from human urine samples of patients with PCa in comparison to those of healthy controls, and analyze lipids in exosomes based on size using nUPLC-ESI-MS/MS. Lipidomic analysis of the two exosome size fractions indicated that the total levels of most lipid groups were increased in patients with PCa to some degree (<2-fold) compared to those in healthy controls. In contrast, levels of DAG, TAG, and ChE were decreased (>2-fold) in patients with PCa compared to healthy controls. However, a decrease in neutral lipids like DAG, TAG, and ChE in PCa exosomes was thought to be due to the increased consumption of energy during the growth of cancer cells. Moreover, these three neutral lipid groups did not represent size dependent decreases in exosomes. While the present work shows the potential to determine exosome sizes and their lipidomic profiles, the future study needs to thoroughly investigate the changes in lipids from different fractions of exosomes of PCa patients, based on a large number of samples.

The preliminary work introduced here not only demonstrated the potential of FIFFF to determine differences in disease status by analyzing sizes of exosome from urine samples

of patients with PCa but also elucidated lipidomic differences in urinary exosome fractions of different sizes collected from PCa patients. High speed and simultaneous determination of the changes in exosome sizes and in lipidomic profiles can be a good combination for the detection of PCa if a proper online method is implemented. This can be integrated to an automated analysis of urine sample by implementing an online concentration device for the isolation and enrichment of exosomes from urine prior to FIFFF. One-step injection of urine sample to an integrated system with FIFFF can bring an automatic sample preparation and size analysis of the exosomes. Moreover, analysis of lipids in exosomes can be directly achieved without the collection of exosomes for lipid extraction by utilizing top-down lipidomic analysis with FIFFF-ESI-MS/MS once lipid targets or markers are established. In this case, it is the desire to preliminary remove urinary proteins external to exosomes to reduce interferences. The current study provided the basis of developing a comprehensive online lipid analysis platform of urinary exosomes by implementing online exosome isolation/purification from urine sample prior to FIFFF followed by the size separation of exosome and simultaneous characterization of exosomal lipids.

## ■ ASSOCIATED CONTENT

### Supporting Information

The Supporting Information is available free of charge on the ACS Publications website at DOI: 10.1021/acs.analchem.6b04634.

Variations of exosome profiles among patients and controls; base peak chromatograms; type of precursor ion/quantifier fragment ion of each lipid class and collision energy used for SRM quantitation and the molecular structure of internal standard with corresponding  $m/z$  values of precursor/quantifier ions in each class; ratio (P/C) of peak area of lipid species between patients and controls; isomeric structures of PC, PE, and TAG species (PDF)

## ■ AUTHOR INFORMATION

### Corresponding Authors

\*Phone: (82) 2 2123 5634. Fax: (82) 2 364 7050. E-mail: mhmoon@yonsei.ac.kr.

\*E-mail: khrha@yuhs.ac.

### ORCID

Myeong Hee Moon: 0000-0002-5454-2601

### Author Contributions

The manuscript was written through contributions of all authors.

### Notes

The authors declare no competing financial interest.

## ■ ACKNOWLEDGMENTS

This study was supported by the grant NRF-2015R1A2A1A01004677 from the National Research Foundation (NRF) of Korea.

## ■ REFERENCES

- (1) Johnstone, R. M.; Adam, M.; Hammond, J. R.; Orr, L.; Turbide, C. *J. Biol. Chem.* **1987**, *262*, 9412–9420.
- (2) Denzer, K.; Kleijmeer, M. J.; Heijnen, H. F. G.; Stoorvogel, W.; Geuze, H. J. *J. Cell Sci.* **2000**, *113*, 3365–3374.

- (3) Kowal, J.; Tkach, M.; Théry, C. *Curr. Opin. Cell Biol.* **2014**, *29*, 116–125.
- (4) Raposo, G.; Stoorvogel, W. *J. Cell Biol.* **2013**, *200*, 373–383.
- (5) Fevrier, B.; Vilette, D.; Archer, F.; Loew, D.; Faigle, W.; Vidal, M.; Laude, H.; Raposo, G. *Proc. Natl. Acad. Sci. U. S. A.* **2004**, *101*, 9683–9688.
- (6) Rajendran, L.; Honsho, M.; Zahn, T. R.; Keller, P.; Geiger, K. D.; Verkade, P.; Simons, K. *Proc. Natl. Acad. Sci. U. S. A.* **2006**, *103*, 11172–11177.
- (7) Record, M.; Carayon, K.; Poirot, M.; Silvente-Poirot, S. *Biochim. Biophys. Acta, Mol. Cell Biol. Lipids* **2014**, *1841*, 108–120.
- (8) Mobius, W.; van Donselaar, E.; Ohno-Iwashita, Y.; Shimada, Y.; Heijnen, H. F.; Slot, J. W.; Geuze, H. J. *Traffic* **2003**, *4*, 222–231.
- (9) Muller, G.; Jung, C.; Straub, J.; Wied, S.; Kramer, W. *Cell. Signalling* **2009**, *21*, 324–338.
- (10) Muller, G.; Schneider, M.; Biemer-Daub, G.; Wied, S. *Cell. Signalling* **2011**, *23*, 1207–1223.
- (11) Caby, M.-P.; Lankar, D.; Vincendeau-Scherrer, C.; Raposo, G.; Bonnerot, C. *Int. Immunol.* **2005**, *17*, 879–887.
- (12) Ranghino, A.; Dimuccio, V.; Papadimitriou, E.; Bussolati, B. *Clin. Kidney J.* **2015**, *8*, 23–30.
- (13) Pisitkun, T.; Shen, R. F.; Knepper, M. A. *Proc. Natl. Acad. Sci. U. S. A.* **2004**, *101*, 13368–13373.
- (14) Welton, J. L.; Khanna, S.; Giles, P. J.; Brennan, P.; Brewis, I. A.; Staffurth, J.; Mason, M. D.; Clayton, A. *Mol. Cell. Proteomics* **2010**, *9*, 1324–1338.
- (15) Miranda, K. C.; Bond, D. T.; Levin, J. Z.; Adiconis, X.; Sivachenko, A.; Russ, C.; Brown, D.; Nusbaum, C.; Russo, L. M. *PLoS One* **2014**, *9*, e96094.
- (16) Welch, H. G.; Albertsen, P. C. *J. Natl. Cancer Inst.* **2009**, *101*, 1325–1329.
- (17) Prensner, J. R.; Rubin, M. A.; Wei, J. T.; Chinnaiyan, A. M. *Sci. Transl. Med.* **2012**, *4*, 127rv3.
- (18) Mitchell, P. J.; Welton, J.; Staffurth, J.; Court, J.; Mason, M. D.; Tabi, Z.; Clayton, A. *J. Transl. Med.* **2009**, *7*, 4.
- (19) Nilsson, J.; Skog, J.; Nordstrand, A.; Baranov, V.; Mincheva-Nilsson, L.; Breakefield, X. O.; Widmark, A. *Br. J. Cancer* **2009**, *100*, 1603–1607.
- (20) Soekmadji, C.; Russell, P. J.; Nelson, C. C. *Cancers* **2013**, *5*, 1522–1544.
- (21) Giddings, J. C. *Science* **1993**, *260*, 1456–1465.
- (22) Litzen, A. *Anal. Chem.* **1993**, *65*, 461–470.
- (23) Nilsson, M.; Wahlund, K.-G.; Bulow, L. *Biotechnol. Tech.* **1998**, *12*, 477–480.
- (24) Lee, H.; Williams, S. K.; Wahl, K. L.; Valentine, N. B. *Anal. Chem.* **2003**, *75*, 2746–2752.
- (25) Reschiglian, P.; Zattoni, A.; Roda, B.; Cinque, L.; Melucci, D.; Min, B. R.; Moon, M. H. *J. Chromatogr. A* **2003**, *985*, 519–529.
- (26) Park, I.; Paeng, K.-J.; Yoon, Y.; Song, J.-H.; Moon, M. H. *J. Chromatogr. B: Anal. Technol. Biomed. Life Sci.* **2002**, *780*, 415–422.
- (27) Rambaldi, D. C.; Zattoni, A.; Casolari, S.; Reschiglian, P.; Roessner, D.; Johann, C. *Clin. Chem.* **2007**, *53*, 2026–2029.
- (28) Barman, B. N.; Ashwood, E. R.; Giddings, J. C. *Anal. Biochem.* **1993**, *212*, 35–42.
- (29) Kang, D.; Oh, S.; Reschiglian, P.; Moon, M. H. *Analyst* **2008**, *133*, 505–515.
- (30) Yang, J. S.; Lee, J. Y.; Moon, M. H. *Anal. Chem.* **2015**, *87*, 6342–6348.
- (31) Kang, D.; Oh, S.; Ahn, S.-M.; Lee, B. H.; Moon, M. H. *J. Proteome Res.* **2008**, *7*, 3475–3480.
- (32) Petersen, K. E.; Manangon, E.; Hood, J. L.; Wickline, S. A.; Fernandez, D. P.; Johnson, W. P.; Gale, B. K. *Anal. Bioanal. Chem.* **2014**, *406*, 7855–7866.
- (33) Sitar, S.; Kežar, A.; Pahovnik, D.; Kogej, K.; Tušek-Žnidarič, M.; Lenassi, M.; Žagar, E. *Anal. Chem.* **2015**, *87*, 9225–9233.
- (34) Byeon, S. K.; Lee, J. Y.; Moon, M. H. *Analyst* **2012**, *137*, 451–458.
- (35) Bang, D. Y.; Lim, S.; Moon, M. H. *J. Chromatogr. A* **2012**, *1240*, 69–76.

- (36) Lim, S.; Byeon, S. K.; Lee, J. Y.; Moon, M. H. *J. Mass Spectrom.* **2012**, *47*, 1004–1014.
- (37) Kitamura, M.; Namiki, M.; Matsumiya, K.; Tanaka, K.; Matsumoto, M.; Hara, T.; Kiyohara, H.; Okabe, M.; Okuyama, A.; Seya, T. *Immunology* **1995**, *84*, 626–632.
- (38) Oksvold, M. P.; Kullmann, A.; Forfang, L.; Kierulf, B.; Li, M.; Brech, A.; Vlassov, A. V.; Smeland, E. B.; Neurauter, A.; Pedersen, K. *W. Clin. Ther.* **2014**, *36*, 847–862.
- (39) Byeon, S. K.; Lee, J. C.; Chung, B. C.; Seo, H. S.; Moon, M. H. *Anal. Bioanal. Chem.* **2016**, *408*, 4975–4985.
- (40) Suburu, J.; Chen, Y. Q. *Prostaglandins Other Lipid Mediators* **2012**, *98*, 1–10.
- (41) Li, J.; Ren, S.; Piao, H.-L.; Wang, F.; Yin, P.; Xu, C.; Lu, X.; Ye, G.; Shao, Y.; Yan, M.; Zhao, X.; Sun, Y.; Xu, G. *Sci. Rep.* **2016**, *6*, 20984.
- (42) Miyanishi, M.; Tada, K.; Koike, M.; Uchiyama, Y.; Kitamura, T.; Nagata, S. *Nature* **2007**, *450*, 435–439.
- (43) Riedl, S.; Rinner, B.; Asslaber, M.; Schaidler, H.; Walzer, S.; Novak, A.; Lohner, K.; Zwegtück, D. *Biochim. Biophys. Acta, Biomembr.* **2011**, *1808*, 2638–2645.